Paper VIII-3 presented at the 1st International Workshop on Progress in Nb-based Superconductors, National Institute for Materials Science, Tsukuba, Japan, Feb. 2-3, 2004. Published in "Progress of Nb-based Superconductors: Proceedings of International Workshop on Nb-Based Superconductors," Ed. K Inoue, T. Takeuchi and A. Kikuchi, pub. Maeda printing Co. Ltd., Japan, pp. 142-149, 2005."

The Properties and Microstructure of Nb-47Ti Superconductor with Magnetic Pinning Centers

L. R. Motowidlo[1], M. K. Rudziak[1], T. Wong[1], L. D, Cooley[2], and P. J. Lee[3]

Supercon, Inc.
Shrewsbury, MA, 01545 USA
[2]Brookhaven National Laboratory
Upton, NY 11973 USA
[3]The Applied Superconductivity Center
UW-Madison, WI53706-1609 USA

ABSTRACT

We have investigated Nb-47Ti multifilament wire with artificial pinning centers (APC). The superconducting properties and proximity effect in wires with ferromagnetic and non-magnetic pins will be discussed. Magnetization and transport measurements will be presented and the pinning characteristics will be discussed as a function of magnetic field, temperature and volume percent pins. In addition, field emission scanning electron microscopy of the pin nanostructure will be presented.

INTRODUCTION

In commercial Nb-47Ti superconductors, high critical current density (J_c) in a magnetic field is achieved by incorporating normal state inclusions that match the vortex density and pin every flux line. The pin nanostructure is produced by applying periodic heat treatments during wire processing to produce non-superconducting alpha-Ti precipitates [1], followed by cold drawing to reduce the precipitates to nanometer thickness (~1-2 nm) and spacing (~3-6 nm). This conventional approach limits the practical alpha-Ti pin volume to approximately 20%.

In the past fifteen years, researchers have also used another approach, artificial pinning centers (APC), to produce very strong nanometer-scale pinning of the vortex lattice [2]. The APC approach allows flexible choice of the pin material, size, and density. In previous studies, the artificial pin materials used were mainly nonmagnetic, and a pin volume fraction up to 50% has been demonstrated [3]. However, due to the so called "proximity effect", the optimum pin volume has been limited to between 20% and 30%. The proximity effect is understood to mean the modification of properties of a superconducting metal, like Nb-Ti, when in intimate contact with a non-superconducting metal, like copper [4,5]. The modification of properties only becomes important when the dimensions or thickness of the superconductor/normal metal (SN) combination are on the order of ≤ 100 nm, such as found in APC microstructures. The consequence of the proximity effect is the reduction of the critical temperature, *(T_c),* and the upper critical field, (H_{c2})*,* which decreases high-field J_c performance in APC Nb-47Ti wires[2]. In addition to

nonmagnetic materials, researchers have also studied ferromagnetic materials such as Fe and Ni artificial pins in Nb-47Ti wires [6, 7]. Ferromagnets (FM) strongly suppress superconductivity, thus a small pin volume can significantly depress the superconducting order parameter and create a large effective pin volume. For example, Nb-47Ti wires containing 2 vol.% Ni pins produced J_c of 2500 A/mm^2 at 5 Tesla comparable to those of commercial Nb-47Ti wire with alpha-Ti pin volume fraction of approximately 21% [7]. More recently, APC strands containing up to 8 vol.% Ni pins with a 4% Cu outer jacket have been studied [8].

In this paper, we compare the superconducting properties and the microstructure of Nb-47Ti conductor containing 12 vol.% (Ni + Cu) ferromagnetic pins to those of conductor containing 12 vol.% Cu nonmagnetic pins to better elucidate the advantages of ferromagnetic materials.

EXPERIMENTAL

Nominally identical superconducting Nb-47Ti multifilament wires containing 12% of either pure Cu or Ni-Cu island type artificial pinning centers were fabricated. In the latter composite, Ni cores were sheathed with Cu such that the volume fractions in the finished APC composite were 8% and 4% and, 6% and 6% respectively. In both pin designs the total pin fraction is 12% of the superconductor fraction in the wire. Multiple restacks were implemented in order to reduce the diameter of the pins by conventional wire drawing to dimensions near diameter and separation of flux lines at 4.2 K. and high fields, approximately 10 nm. Details of preparation and fabrication of these APC wires have been presented elsewhere [8]. A summary of the APC conductor design characteristics and pin characteristics is presented in TABLE 1.

In FIGURE 1, a scanning electron image at an intermediate processing stage of the APC composite shows a hexagonal arrangement of the island type artificial pins. The initial stack of 91 island pins shown in FIGURE 1 is surrounded by a niobium barrier. For samples 2A4, 3A4, and 4A4, the copper sheath is chemically etched off the first 91 stack, and the subsequent restack of 91×61 results in 5,551 pins in a final filament diameter of approximately 1.8 μm. The total number of filaments within the copper wire matrix for both samples is 3,721. For sample 3A4-2, the copper was again removed prior to the third stack, resulting in 61 filaments with diameter 16.7 μm and $61^2 \times 91 = 338{,}611$ pins. The calculated pin diameter, shown in TABLE I, is for the optimum wire diameter at which peak J_c was obtained at 5 T. An SEM image of an island pin in sample 3A4-2 is shown in FIGURE 2. In this case, the pin design includes 8% Ni surrounded by 4% Cu. We observe that the interface between the Ni and Cu is smooth, which is probably due to the availability of many slip planes for the fcc crystal structures of both materials.

TABLE I

Sample ID	Wire φ (mm)	#Fil.	SC vol.%	Fil.. Φ(μm)	Pin Comp.	Pin[a] Φ (nm)
2A4	0.279	3721	16.73	1.87	12Cu	9.13
3A4	0355	3721	9.68	1.81	8Ni4Cu	8.84
4A4	0.279	3721	17.93	1.94	6Ni6Cu	9.47
3A4-2	0.327	61	15.90	16.72	8Ni4Cu	10.45

[a]Calculated pin diameter.

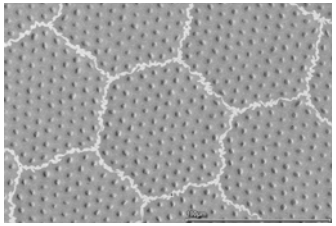

FIGURE 1. SEM image of an APC composite containing island pins.

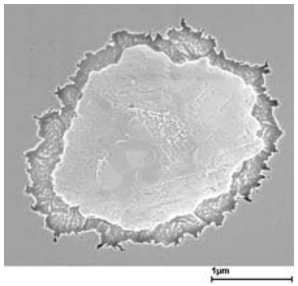

FIGURE 2. SEM image of an (8Ni/4Cu) APC pin in a Nb-47Ti matrix.

However, the interface between Cu and a very thin Nb diffusion barrier separating the copper from the Nb-47Ti matrix is rough. This is believed to reflect the deformation characteristics of bcc Nb materials [9]. This may eventually lead to the higher aspect ratio of the Cu pins versus Ni+Cu pins.

The superconducting properties were characterized by a vibrating sample magnetometer (VSM) and standard transport measurements. Magnetization measurements as a function of temperature and applied magnetic field were performed at the University of Wisconsin-Madison (UW) to determine the Bulk Pinning Force *(F_p)*, the Irreversibility field *(H*)*, H_{c2}, and T_c. In addition, transport measurements were performed at Supercon, Inc. using the four point method at 4.2 K in applied magnetic fields up to 9 T on both short and barrel samples. A voltage criteria of 10^{-12} Ω·cm was used to determine J_c. The magnetization measurements were performed on as-drawn wire samples in perpendicular field. Transport measurements were performed on short samples in the as-drawn condition and after annealing at temperatures from 100°C to 700°C for 1 minute to 20 minutes. All samples were characterized at the final diameter specified in TABLE I Samples at various stages of the wire processing and pin size were also prepared and mounted for field emission scanning electron microscopy (FESEM) at UW. These samples were studied in both as drawn and annealed conditions.

RESULTS AND DISCUSSION

The Effect of Pinning Material on F_p

The bulk pinning force, F_p, as a function of the applied magnetic field was determined from transport measurements. In FIGURE 3, we compare F_p for APC wires with 8Ni/4Cu, Nb and Cu pins. For all three pin designs, the pin fraction was 12 vol.%. We find significant improvement in F_p with the applied magnetic field for APC wires containing the 8Ni/4Cu pins as compared to APC wires with non-magnetic pins. For example at 5 Tesla, F_p is approximately 40% higher with FM pins than wires designed with non-magnetic pins. The results demonstrate the effectiveness of the FM pins.

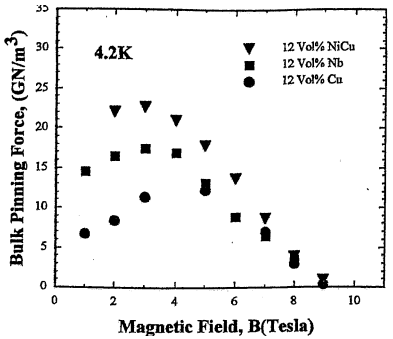

FIGURE 3, The bulk pinning force as a function of the applied magnetic field for wires with Ni/Ci, Nb, and Cu pin designs.

It is believed that complete suppression of superconductivity by Ni/Cu pins results in strong core pinning. Another possible contribution for the effective flux pinning of the Ni/Cu pins in the present result, may be from the interaction of the magnetic moment of FM pins and the magnetic field of the flux lattice.[10] For the wires with non-magnetic Nb and Cu pins, we observe similar F_p characteristics at applied magnetic fields > 5 Tesla. Below 5 Tesla however, the APC wires with Nb diverges from the F_p characteristics of APC wires with Cu, The significant F_p enhancement has been discussed in terms of a repulsive Nb pinning center that depends sensitively on the larger coherence length of the Nb pins[11].

The Filament Size Effect on F_p

In FIGURE 4, we present the F_p characteristics for 8Ni/4Cu pins with identical pin diameters but with final filament diameters (~1.8 μm vs. ~16.7 μm). While the pins are at optimum diameters of ~ 10 nm in both cases, the F_p(5 T) as determined from transport measurements for 8Ni/4Cu design with ~ 16.7 μrn filaments is ~ 22% higher at 4.2 K. The result suggests that the filament size and the proximity effect of the surrounding copper matrix is an important design consideration. The result is consistent with past results on Nb-47Ti composites with sub-micrometer filaments [12,13].

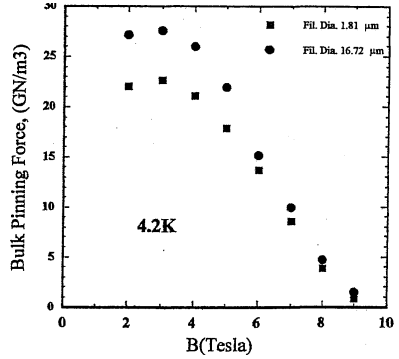

FIGURE 4. The bulk pinning force as a function of the applied magnetic field for similar pin design (8Ni/4Cu) but with different final filament diameters.

The Scaling Behavior of APC Wires with Magnetic and non-Magnetic Pins

The temperature and magnetic field dependence of APC wires with magnetic and non-magnetic pins was obtained by magnetization measurements. In FIGURES 5 and 6 the reduced bulk pinning force, F_p/F_{pmax}, as function of the reduced magnetic field b(B_{c1}/H_{c2}) at different temperatures from 4.2 K to 8 K is presented. For the optimized (8Ni/4Cu) APC wire, good scaling behavior of the reduced pinning curves is observed at various temperatures. The peak in the reduced F_p occurs at b = 0.28 and the reduced field dependent pinning curve function is approximately $b^{0.5}(1\text{-}b)$. The inset in FIGURE 5, shows F_{pmax} as a function of the temperature dependent H_{c2}. The slope of this curve for the temperature dependent H_{c2} term of the scaling law is equal to 1.9. In the case of the APC wire with Cu pins, a lack of scaling is observed. The peak in the reduced F_p occurs at b = 0.35 at 7 K and shifts to 0.5 at 4.2 K. This is a similar behavior observed in highly aspected α-Tí pins found in conventionally processed wires[14]. In the present case while not as severe as in the ribbon like α-Ti pins, APC wires with Cu pins display an aspected geometry (see Figure 7a and 7b) as compared to APC wires containing Ni/Cu pins. This may explain the difference in the reduced F_p characteristics.

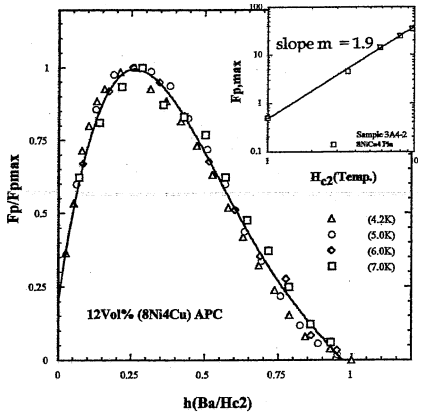

FIGURE 5. The normalized pinning characteristics of APC wire with ferromagnetic Ni/Cu pins.

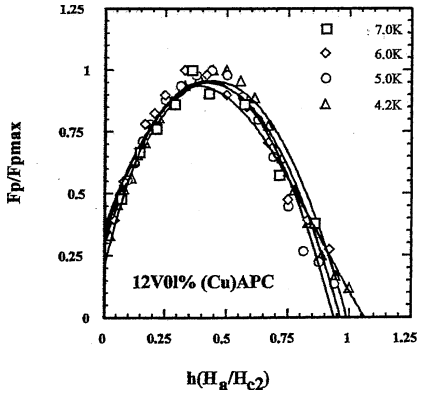

FIGURE 6. The normalized pinning characteristics of APC wire with Cu pins.

The Upper Critical Field and Transition Temperature

The upper critical field, H_{c2}(4.2 K), and the Irreversibility field, H^*(4.2 K), were determined from magnetization loops. H_{c2} is obtained where the slope of the reversible magnetization curve reverts to that of the background paramagnetic state. H^* is obtained at the point where the magnetization hysteresis loop closes. The transition temperature of the samples was also determined from the change in slope of the magnetic moment. The results are summarized for the respective APC designs in TABLE 2. If we compare the APC designs with 2A4 and 3A4, we find that the H_{c2}, H^*, and T_c results are comparable. However, when the final filament diameter is increased in 3A4-2 the superconducting characteristics are improved. The obtained values for design 3A4-2 in TABLE 2 are the best superconducting properties for any APC composite made to date, and approach those of conventional Nb-47Ti. This is further support for the fact that the performance of small diameter (~1.8 μm) filaments is reduced due to the proximity effect with the external Cu sheath.

TABLE II

Sample ID	H_{c2}(4.2 K)	H^*(4.2 K)	T_c(K)
2A4	9.8	9.0	8.30
3A4	9.8	9.1	7.95
4A4	10.2	9.7	8.60
3A4-2	11.0	9.8	8.45

Scanning Electron Microscopy of Magnetic and Non-Magnetic Pins

FESEM analysis of design 2A4 at 1.37 mm diameter and design 3A4-22 at 2.26 mm diameter were performed. The respective nano-structures shown in FIGURE 6 are at 5 to 7 times larger than the optimum pin diameters as determined by transport measurements. The pin nano-structure for design 2A4 after applying anneals equivalent to 3 minutes at 187°C, is shown in FIGURE 7a. We observe elongated dark regions up to 100 nm long and 10 nm to 20 nm thick. In contrast, the nano-structure shown in FIGURE 7b for sample 3A4-2 shows rounder 8Ni4Cu pins that have maintained a uniform distribution of the original hex design pattern.

In addition, curious dark areas around the outside of the Ni-Cu pins are visible. We consider the dark regions to be the possible formation of voids due to inter-diffusion of the Ni-Cu interface. The formation of voids in the Cu pin design may be due to inter-diffusion of Cu atoms with Ti atoms from the matrix. In previous work on Cu-Nb-NbTi interfaces of NbTi filaments, researchers found by electron microprobe analysis and scanning auger microprobe that Cu diffuses further and faster into the NbTi matrix than Ti into the Cu matrix [15,16]. Consequently, voids may form on one side of the diffusion couple. The diffusion distances in the present study are only on the order of nanometers. In addition, the total strain seen by the pins due to cold work is about 8. Thus, the stored mechanical energy should be sufficient to enhance rapid inter-diffusion.

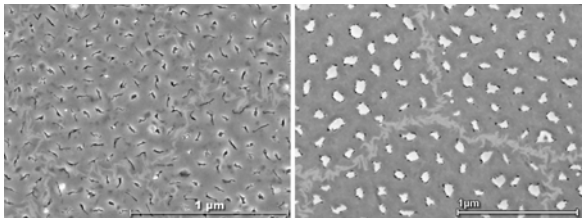

FIGURE 7. FESEM of annealed a) APC design 2A4-1 (Cu pins) and b) design 3A4-2

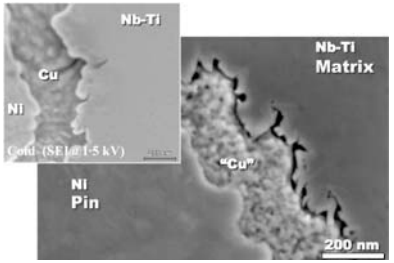

FIGURE 8. SEM image of pins with inset detail showing extended void formation after annealing at 175°C for 15 minutes.

In the 8Ni4Cu pin design, inter-diffusion may also occur between the Ni and Cu atoms forming a Cu-Ni alloy barrier with significantly higher resistivity [17]. To further investigate this feature, additional imaging was performed on samples with larger 8Ni4Cu pins annealed at 175°C for 15 minutes. The base image in FIGURE 8 is of the pins in the annealed samples, while the insert shows the microstructure of the un-annealed pin. This comparison reveals void formation on the outer edges of the copper barriers in the annealed sample.

The formation of a highly resistive barrier may explain the improved J_c performance of 3A4-2 by reducing the proximity effect and thus increasing the effectiveness of the pinning volume. The combination of a more intact ferromagnetic core and a high resistivity barrier allows for fabrication of pins that is beneficial at high magnetic fields.

CONCLUSIONS

We have fabricated multifilament Nb-47Ti wires with magnetic Ni-Cu and non-magnetic pure Cu artificial pinning centers. The F_p properties were investigated using magnetization and transport measurements. For as-processed APC wires the F_p*(5T,42 K)* results for magnetic APC are about 40% higher than those of an otherwise identical wire with pure Cu pins. Designs with final filament diameters of about 1 µm also suffered from proximity coupling to the external copper matrix, and further improvement, ~22%, in the performance of magnetic APC wires was seen for increasing the filament diameter to ~17 µm while keeping the nanostructural dimensions the same. This latter design exhibited an upper critical field of 11.0 Tesla at 4.2 K, the highest of any APC composite made so far. Low temperature heat treatments were also applied to the APC designs studied in this paper. We found that a pin design combination of ferromagnetic nickel with a copper barrier after low temperature (100°C to 300°C) annealing results in

4500 to 5000 A/mm^2 at 5 T, 4.2 K, Field-emission scanning electron microscopy conducted on samples from somewhat larger wire diameter showed that voids are formed on the outside of each pin as a result of inter-diffusion. In the case of the copper pins, voids are found to form within the pins after low temperature heat treatment. Further improvement in the J_c performance in APC Nb-47Ti is expected by increasing the pin volume percentage and optimizing the void formation.

ACKNOWLEDGMENTS

The authors would like to thank Mr. *J.* Fernandez for the transport measurements at Supercon, Inc. This work was partially supported by the U.S. Department of Energy under Grant No. DE-FG02-01ER83327 (Department of High Energy Physics),

REFERENCES

1. Lee, P.J. and Larbalestier, D.C., In *Concise Encyclopedia of Magnetic & Superconducting Materials,* Editor, Jan Evetts, Publisher, Pergamon Press 1992, pp, 357-363.
2. Cooley, L. D. and Motowidlo, L. R., *Supercond. Sci. Technol,* vol. 12, pp. R135-R151,(1999).
3. Motowidlo, L.R., Kanithi, H.C., and Zeitlin, B.A.,"NbTi Superconductors with Artificial Pinning Centers", in *Adv. in Cryo. Eng.,36A,* edited by R.P. Reed and F.R. Fickett, Plenum Press NY,199G, pp.311-316.
4. DeGennes, P. G., "Boundary effects in superconductors," *Rev. of Mod. Phys.,* vol. 36, pp. 225-237, January 1964.
5. Levi, Y., Millo, O., Rizzo, N. D., Prober, D. E., and Motowidlo, L. R., *Phys. Rev. B,* Vol.58, No.22, pp. 15 128-15 134, (1998).
6. Cooley, L. D., Jablonski, P. D., Heussner, R. W. and Larbalestier, D. C., "Nb-Ti wires with artificial ferromagnetic pins," in *Adv. in Cryo. Eng., 42,* L. T. Summers, Ed., NY,Plenum, 1996, pp. 1095-1102.
7. Rizzo, N. D., Wang, J. Q., Prober, D. E., Motowidlo, *L.R.*, and Zeitlin, B. A., *Appl Phys. Lett.,Vol* 69,No. 15, pp. 2285-2287, (1996).
8. Motowidlo, L.R., Rudziak, M. K., Wong, T.,"The pinning strength and upper critical fields of magnetic & nonmagnetic APC's in Nb-47Ti wires", *IEEE Tram. Appl Supercond.,* Vol.13,2, 2003, pp.3351-3354.
9. Thornton, P.A. and Colangelo, V.J., *Fundamentals of Engineering Materials*, Publisher, Prentice Hall, 1985.
10. Wang, J.Q., Rizzo, N.D., Prober, D.E., Motowidlo, L.R., and Zeitlin, B.A., *IEEE Trans. Appl. Supercond*. Vol.7,2, l997, pp.1130
11. Matsushita,T., *et al*, in *Adv. Cryo. Eng.,*42, L.T. Summers, Ed., NY, Plenum, 1996, *pp.* 1103-1108.
12. X. S. Ling, J. D. McCambridge, D. E. Prober, L. R. Motowidlo, B. A. Zeitlin, and M S. Walker, "Flux dynamics in submicron superconducting NbTi wires," *Physica B,* vol. 194-196, pp. 1867-1868, 1994.
13. Hlasnik, L., *et al., Cryogenics*, Vol. 25, p. 558, (1985).
14. Meingast, C. and Larbalestier, D.C., *J.Appl Phys.,* 66, (1992) 2964.
15. Larbalestier, D.C., Lee, P.J., and Samuel R.W., "The growth of intermetallic compounds at a copper-niobium-titanium interface", *in. Adv. in Cryo. Eng.,* 32, edited by R.P. Reed and A.F. Clark, Plenum Press NY, 1986, pp.715-722.
16. Faase, K.J., Lee, P.J., Mc Kinnell, J.C., and Larbalestier, D.C., "Diffusional reaction rates through the Nb wrap in SSC and other advanced multifilamentary Nb-47Ti composites", in *Adv. in Cryo. Eng.,38B.,* edited by F.R. Fickett and R.P. Reed, Plenum Press NY, 1992, pp.723-730.
17. Lee, P.J., Larbalestier, D.C., Motowidlo, L.R., Rudziak, M. K., and Wong, T., These proceedings, *ICMC 2003 Conference,* Paper (M1-R-04).
18. Guy, A.G., *Introduction to Materials Science,* B. J. Clark and Peter Karsten, Eds., New York: McGraw-H3I,1971, pp. 265-269.